

Coupled $S = \frac{1}{2}$ Heisenberg antiferromagnetic chains in an effective staggered field

Masahiro Sato and Masaki Oshikawa

Department of Physics, Tokyo Institute of Technology, Oh-okayama, Meguro-ku, Tokyo 152-8550, Japan

(Received 16 June 2003; revised manuscript received 10 November 2003; published 12 February 2004)

We present a systematic study of coupled $S = 1/2$ Heisenberg antiferromagnetic chains in an effective staggered field. We investigate several effects of the staggered field in the *higher (two or three) dimensional* spin system analytically. In particular, in the case where the staggered field and the interchain interaction compete with each other, we predict, using mean-field theory, a characteristic phase transition. The spin-wave theory predicts that the behavior of the gaps induced by the staggered field is different between the competitive case and the noncompetitive case. When the interchain interactions are sufficiently weak, we can improve the mean-field phase diagram by using chain mean-field theory and the analytical results of field theories. The ordered phase region predicted by the chain mean-field theory is substantially smaller than that by the mean-field theory.

DOI: 10.1103/PhysRevB.69.054406

PACS number(s): 75.10.Jm

I. INTRODUCTION

The effects induced by magnetic fields in magnets have been a subject of theoretical research interest for a long time. In particular, recently the magnetization processes of various spin chains and ladders have been investigated intensively. Owing to the progress of the various experimental methods, there has been an increasing connection between the theories and the experiments. In such a context, one of the new attractive subjects in magnetism is the effects of a *staggered* magnetic field, namely, a magnetic field which changes direction alternately. While it may sound unrealistic, there exist at least three mechanisms generating the staggered fields in real magnets, as discussed in Refs. 1 and 2.

The first mechanism is due to the staggered gyromagnetic (g) tensor, which can be present if the crystal structure is not translationally invariant. The staggered g tensor $g_{\alpha\beta}^{st}$ is defined in the coupling between the spin and the external magnetic field (Zeeman term) as

$$\hat{H}_{\text{Zeeman}} = -\mu_B \sum_j H_\alpha [g_{\alpha\beta}^u + (-1)^j g_{\alpha\beta}^{st}] S_j^\beta, \quad (1)$$

where $\vec{H} = (H_x, H_y, H_z)$ is an applied uniform magnetic field and S_j^β is the spin operator of the local magnetic moment. Here $H_\alpha g_{\alpha\beta}^{st}$ is nothing but an effective staggered field. In addition, the staggered field may also arise from the staggered Dzyaloshinskii-Moriya (DM) interaction^{3,4}

$$\hat{H}_{\text{DM}} = \sum_j (-1)^j \vec{D} \cdot (\vec{S}_j \times \vec{S}_{j+1}), \quad (2)$$

which can be present if the crystal symmetry is sufficiently low. It is shown in Refs. 1 and 5 that in the presence of the staggered DM interaction along the chain, an applied uniform field \vec{H} also generates an effective staggered field $\vec{h} \propto \vec{D} \times \vec{H}$. Several quasi-one-dimensional Heisenberg antiferromagnets are now known to have the staggered field due to the above mechanisms. The well-known examples are Cu-benzoate,⁶⁻⁸ $[\text{PM} \cdot \text{Cu}(\text{NO}_3)_2 \cdot (\text{H}_2\text{O})_2]_n$ (PM = pyrimidine),⁹ and Yb_4As_3 .¹⁰⁻¹² All of these have low-

symmetry crystal structures which allow a staggered g tensor and a DM interaction along the chain.¹³ It is expected in Refs. 1, 5, and 14 that the staggered field induces an excitation gap in the $S = 1/2$ Heisenberg antiferromagnetic (HAF) chain, which should be otherwise gapless. The excitation gap caused by the staggered field is indeed found in these materials.^{6,9,12} Moreover, low-temperature anomalies in physical quantities, such as the susceptibility and the electron spin resonance linewidth,^{15,16} are also successfully explained as effects of the staggered field.⁵ Thus it is confirmed that they are described by an $S = 1/2$ HAF model with an effective staggered field.

There is another, rather different, mechanism to generate a staggered field. Let us suppose that the system consists of two sublattices, with a weak interlattice coupling and strong intralattice one. If one of the sublattices is Néel ordered, the interlattice coupling, as a mean field, could give an effective staggered field on the other sublattice. The realization of this scenario is in $R_2\text{BaNiO}_3$ where R is a magnetic rare earth, and the R -ion lattice provides a staggered field for Ni chains ($S = 1$).^{17,18}

Actually all the materials discussed above are highly one-dimensional (1D). However, at lower temperature and lower energy, the interchain interaction will eventually be dominant. In addition, there are reports on a few materials [$\text{CuCl}_2 \cdot 2\text{DMSO}$ (DMSO = dimethylsulphoxide) (Refs. 19–21) and $\text{BaCu}_2(\text{Si}_{1-x}\text{Ge}_x)_2\text{O}_7$ (Ref. 22)] which seem to have an effective staggered field and also a relatively large interchain interaction. Therefore the work including the interchain interaction could be relevant for experiments.

Given these backgrounds, in the present paper, we would like to clarify the characteristic roles of staggered fields in *higher-dimensional* spin systems. In this paper, we are concerned with dimensions *higher than 1* but still realistic in condensed-matter physics, namely, *two or three* dimensions. However, most of the analyses in this paper apply straightforwardly even to four dimensions or higher.

Varieties of spin models with effective staggered fields are conceivable. As a simplest model including both the staggered field and the interchain coupling, in this paper, we concentrate on the following $S = 1/2$ spatially anisotropic Heisenberg Hamiltonian:

$$\hat{H} = \sum_r (J \vec{S}_{i,j,k} \cdot \vec{S}_{i+1,j,k} + J_{\perp} \vec{S}_{i,j,k} \cdot \vec{S}_{i,j+1,k} + J'_{\perp} \vec{S}_{i,j,k} \cdot \vec{S}_{i,j,k+1}) - H \sum_r S_{i,j,k}^z - h \sum_r (-1)^i S_{i,j,k}^x, \quad (3)$$

where $\vec{S}_{i,j,k}$ is the spin 1/2 operator on $\vec{r} = (i,j,k)$ site. The coupling constants are restricted to $J > |J_{\perp}| \geq |J'_{\perp}|$, and thus the i direction is the strongly antiferromagnetic (AF) coupled one. The system with $J'_{\perp} = 0$ is 2D, in which the index k vanishes. The last two terms represent the uniform and staggered Zeeman terms, respectively.

In our model (3), one can immediately find that when the interchain interactions are AF, they compete with the staggered Zeeman energy, while in the ferromagnetic (FM) case, both the interactions and the staggered field h jointly make a Néel state stable. Let us refer the AF case as the *competitive* case, and the FM case as the *noncompetitive* one. As will be explained later on, we predict that the competition brings a second-order phase transition in the competitive case. Its emergence is one of the most characteristic effects of the staggered field in our higher-dimensional spin model.

The rest of this paper is organized as follows. In Sec. II, we apply mean-field theory to the model (3). In the competitive case a phase transition is predicted. Since we are primarily interested in the transition, which is characteristic for the higher-dimensional system, in the later sections we will mainly discuss the competitive case. The noncompetitive case is touched as a comparison to the competitive case. Besides the phase diagrams, the mean-field magnetization curves and critical exponents are derived from the self-consistent equations. In Sec. III, using linear spin-wave approximation, we derive the spin-wave dispersions in the competitive case and in the noncompetitive case. As a result, we find that the excitation gap induced by the staggered field behaves differently between the competitive case and the noncompetitive case.

In Sec. IV, we improve the mean-field phase diagrams by using chain mean-field theory.^{23,24} The latter is expected to be superior, when the interchain interactions are weak and the effective 1D model can be solved exactly. The improved diagram shows that in the weakly coupling region of the competitive case, the ordered phase becomes much narrower than the mean-field prediction. In the last section, we summarize those results and discuss future problems. In the Appendix, the details of the spin-wave results are given.

II. MEAN-FIELD THEORY APPROACH

In this section, we treat the model (3) within mean-field theory (MFT) framework. We first discuss the competitive case, and then touch the noncompetitive case briefly.

In the competitive case, considering the advantage of both the interchain energy and the staggered Zeeman energy as well as the intrachain coupling J , we can expect that the spin moment turns as Fig. 1 at sufficiently low temperature and

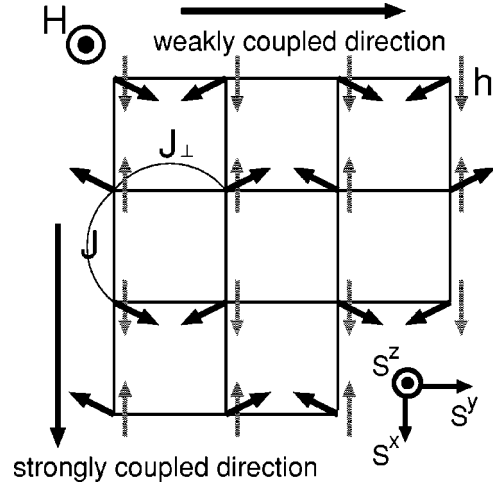


FIG. 1. Directions of the magnetic fields and the spin moments in the 2D competitive case. The short black arrows are the spin moments projected onto spin xy plane in the ordered phase (spontaneous symmetry breaking phase, see text) expected by the MFT. The gray arrows indicate the direction of the staggered field h . The uniform field H is applied perpendicular to this paper.

small fields comparable to the interchain couplings. The assumed spin moment is

$$\langle \vec{S}_{i,j,k} \rangle_{\text{MFT}} = ((-1)^i m_x, (-1)^{i+j+k} m_y, m_z). \quad (4)$$

The choice of the mean field (4) is presumably valid as long as J is sufficiently larger than J_{\perp} and J'_{\perp} . On the other hand, for instance, in the limiting case: $J \rightarrow 0$, where the model is reduced to a 2D or 1D AF one with a uniform field, there are possibilities that $\langle S_{j,k}^{x,z} \rangle$ are inhomogeneous along the j or k directions, and thus Eq. (4) is invalid. In this paper, the MFT in the competitive case is performed only within the mean field (4).

The minimal condition for the mean-field free energy gives the following self-consistent equations:

$$m_x = \frac{\epsilon_x}{2\epsilon} \tanh(\beta\epsilon), \quad (5a)$$

$$m^2 = \frac{1}{4} \tanh^2(\beta\epsilon), \quad (5b)$$

where

$$\epsilon_x \equiv (J - J_{\perp} - J'_{\perp}) m_x + h/2,$$

$$\epsilon_y \equiv (J + J_{\perp} + J'_{\perp}) m_y,$$

$$\epsilon_z \equiv -(J + J_{\perp} + J'_{\perp}) m_z + H/2,$$

$$\epsilon \equiv (\epsilon_x^2 + \epsilon_y^2 + \epsilon_z^2)^{1/2}, \quad (6)$$

and β and m are, respectively, the inverse temperature $1/k_B T$ and the total magnetization per site. The numerical solutions of Eq. (5a) are given in Fig. 2. They indicate that there is a second-order phase transition, and the corresponding order parameter is the y component of the spin moment, $m_y = |\langle S_{i,j,k}^y \rangle|$. Going back to Fig. 1, one sees that the phase with finite m_y breaks the translational symmetry in the

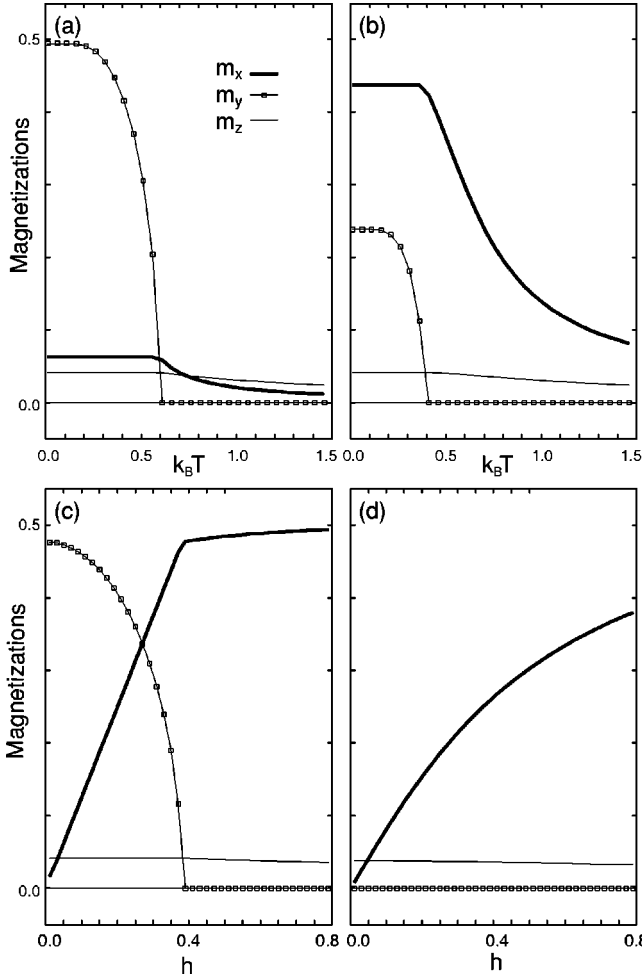


FIG. 2. Magnetization curves of the competitive case for $(J, J_{\perp} + J'_{\perp}, H) = (1, 0.2, 0.2)$. These are obtained by the numerical iterative method for Eq. (5a). The upper two parts (a) and (b) are in $h = 0.05$ and $h = 0.35$, respectively. The lower two parts (c) and (d) are in $k_B T = 0.3$ and $k_B T = 0.7$, respectively.

weakly coupled direction. In the following, we call this phase as the SSB (spontaneous symmetry breaking) phase. The other phase, in which the spins are aligned to the field with $m_y = 0$, will be called as the *symmetric* phase. We emphasize that the transition between these two phases occurs only in the high-dimensional spin systems and in the presence of the competition. From these results, we can illustrate the variation of the spin moment when the staggered field h is increased gradually at small T and H with Fig. 3.

In the SSB phase, the relations $m_x = h/[4(J_{\perp} + J'_{\perp})]$ and $m_z = H/[4(J + J_{\perp} + J'_{\perp})]$ hold within the MFT. Inserting these into Eq. (5b) and taking the limit $m_y \rightarrow 0$, we obtain the mean-field critical surface in the space $(k_B T, H, h)$:

$$\tilde{h}_c^2 + \tilde{H}_c^2 = \frac{1}{4} \tanh^2 \{ \beta_c (J + J_{\perp} + J'_{\perp}) \sqrt{\tilde{h}_c^2 + \tilde{H}_c^2} \}, \quad (7)$$

where $\tilde{h}_c \equiv h_c/[4(J_{\perp} + J'_{\perp})]$, $\tilde{H}_c \equiv H_c/[4(J + J_{\perp} + J'_{\perp})]$ and the subscript c represents critical values. It can be simplified in the cases $T = 0$, $h = 0$, and $H = 0$, respectively, as

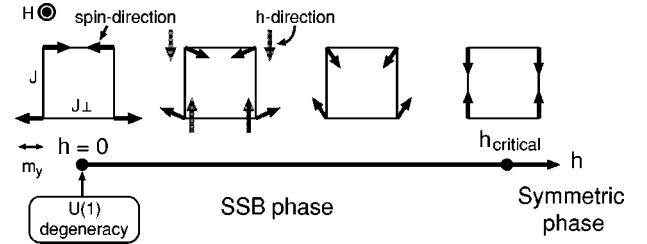


FIG. 3. Variation of the spin configuration in a plaquette when the staggered field is increased gradually in the 2D competitive case. The black arrows represent spin directions projected onto spin xy plane. The gray arrows are the staggered field h .

$$\tilde{h}_c^2 + \tilde{H}_c^2 = \frac{1}{4},$$

$$\tilde{H}_c = \frac{1}{2} \tanh \left(\frac{\beta_c H_c}{4} \right),$$

$$\tilde{h}_c = \frac{1}{2} \tanh \{ \beta_c (J + J_{\perp} + J'_{\perp}) \tilde{h}_c \}. \quad (8)$$

Thus the mean-field phase diagram can be represented as Fig. 4. Using the critical condition, one can calculate some critical exponents within the MFT. Near the critical surface in the SSB side, the order parameter, the off-diagonal uniform and staggered susceptibilities, $\chi_u \equiv \partial m_y / \partial H$ and $\chi_s \equiv \partial m_y / \partial h$, behave, respectively, as $m_y \sim (A_c - A)^\beta$, $\chi_u \sim -(A_c - A)^\gamma$, and $\chi_s \sim -(A_c - A)^{\gamma'}$ where A stands for T , H , or h . The critical exponent β is found to be the conventional mean-field value $1/2$. On the other hand, both γ and γ' turns out to be $1/2$, which is different from the standard MFT result 1. This is because m_y is perpendicular to H and h , and thus the latter are not the conjugate field as in the standard case. The mean-field energy per site is given as

$$\epsilon_{\text{MFT}} = - \{ J(m_x^2 + m_y^2 - m_z^2) + H m_z + h m_x + (J_{\perp} + J'_{\perp})(m_y^2 - m_x^2 - m_z^2) \}. \quad (9)$$

From this, one can easily confirm that the critical exponent for the specific heat is zero.

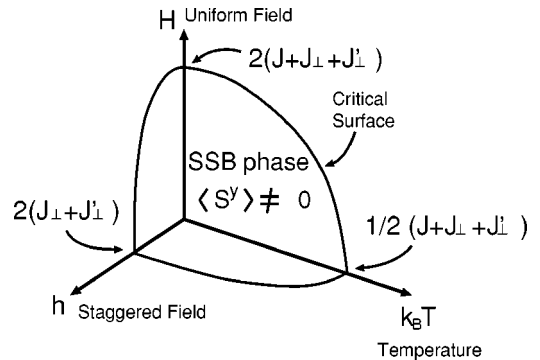


FIG. 4. Schematic mean-field phase diagram in the competitive case.

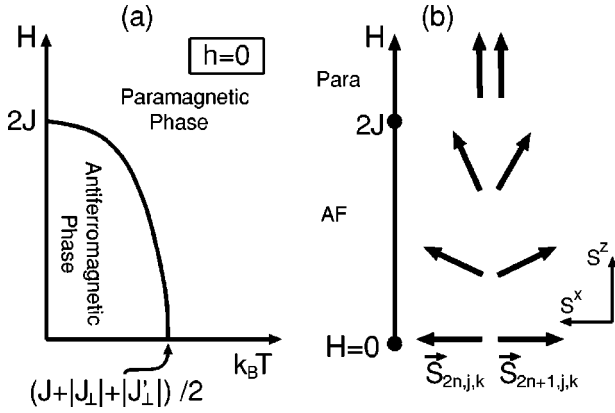


FIG. 5. (a) Schematic mean-field phase diagram of the noncompetitive case in $h=0$. (b) The variation of the spin moment when the uniform field is increased gradually in $h=T=0$.

Now, we turn to the noncompetitive case. Because of no competitions, no singular phenomena occur when $h \neq 0$. Canting of the spins in zx plane lowers both the interchain interactions and the Zeeman energies. Thus the expectation value of the spin moments can be put as

$$\langle \vec{S}_{i,j,k} \rangle_{\text{MFT}} = ((-1)^i m_x, 0, m_z). \quad (10)$$

The MFT in this case gives the self-consistent equations $m_{x(z)} = (\epsilon'_{x(z)}/2\epsilon') \tanh(\beta\epsilon')$ where $\epsilon'_{x(z)} \equiv [(-)J + |J_\perp| + |J'_\perp|] m_{x(z)} + h(H)/2$ and $\epsilon' \equiv (\epsilon_x^2 + \epsilon_z^2)^{1/2}$. At $h=0$, the system reduces to a conventional AF magnet in a uniform magnetic field. Hence, there must be a phase transition which divides the AF and paramagnetic phases, characterized by the order parameter m_x . The critical line is given by

$$\frac{H_c}{4J} = \frac{1}{2} \tanh \left\{ \beta_c (J + |J_\perp| + |J'_\perp|) \frac{H_c}{4J} \right\}. \quad (11)$$

The phase diagram and the variation of the spin moment are drawn in Fig. 5. In the three-dimensional parameter space $(k_B T, H, h)$, the AF phase gives a first-order phase transition plane.

III. LINEAR SPIN-WAVE APPROXIMATION IN $T=0$

With the MFT described in the preceding section, we investigate the effects of the quantum fluctuations in both the competitive and the noncompetitive cases, at $T=0$. The standard linear spin-wave approximation, based on the Holstein-Primakoff transformation (HPT) (Ref. 25) is employed. The detailed results are given in the Appendix.

First we discuss the SSB phase of the competitive case, which is the main subject. In the HPT, we replace the spin operator with a boson annihilation (creation) operator c (c^\dagger) as follows:

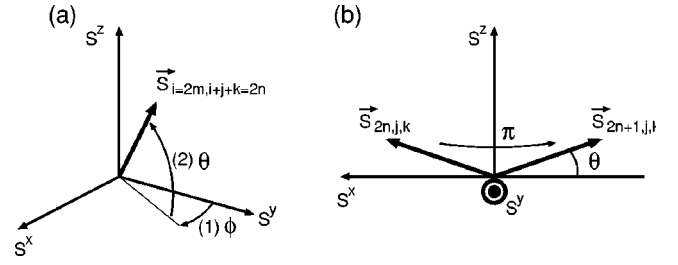


FIG. 6. The definitions of the canting parameter. In the SSB phase, as in (a), each spin direction is given by two rotations (1) $R_z(-\phi)$ and (2) $R_x(\theta)$ applied in this order to spin pointing to y direction. In the symmetric phase or in the noncompetitive case, spins are canted in the zx plane as shown in (b).

$$\vec{S}_{\text{HP}} = \begin{pmatrix} i \sqrt{\frac{S}{2}} \left(1 - \frac{c^\dagger c}{2S} \right) (c^\dagger - c) \\ S - c^\dagger c \\ \sqrt{\frac{S}{2}} \left(1 - \frac{c^\dagger c}{2S} \right) (c^\dagger + c) \end{pmatrix} \approx \begin{pmatrix} i \sqrt{\frac{S}{2}} (c^\dagger - c) \\ S - c^\dagger c \\ \sqrt{\frac{S}{2}} (c^\dagger + c) \end{pmatrix}, \quad (12)$$

where S is the spin quantum number generalized from $S=1/2$ and the sign \approx denotes the leading approximation in the $1/S$ expansion. The above HPT is useful if the spin points to the y direction in the classical ground state, as the bosons then represent quantum fluctuations.

In the SSB phase, actually, a canting structure (4) is expected in the classical ground state, which is equivalent to the MFT at $T=0$. The canted spin moments may be expressed by the angles (θ, ϕ) as

$$\langle \vec{S}_{i,j,k} \rangle = m \begin{pmatrix} (-1)^i \cos \theta \sin \phi \\ (-1)^{i+j+k} \cos \theta \cos \phi \\ \sin \theta \end{pmatrix}. \quad (13)$$

Thus in order to apply the HPT to the present case, we use the representation

$$\vec{S}_{i,j,k} \rightarrow R_x((-1)^{i+j+k} \theta) \times R_z((-1)^{j+k}(-\phi) + \delta_{i+j+k, \text{odd}} \pi) \vec{S}_{\text{HP}}, \quad (14)$$

where the operator $R_\alpha(\beta)$ represents a rotation about α axis by angle β . The operation (14) is described in Fig. 6. For the original spin model (3), these rotations correspond to a unitary transformation. After these transformations, the leading-order terms in $1/S$ is retained to give a solvable Hamiltonian which is quadratic in bosonic operators.

The canting angles of the classical ground state are given by minimizing the classical Hamiltonian, which is equivalent to the MFT energy, Eq. (9). The canting angles in the classical ground state are thus given as

$$\cos \phi_{\text{cl}} \sin \theta_{\text{cl}} = \frac{H}{4S(J + J_\perp + J'_\perp)}, \quad (15)$$

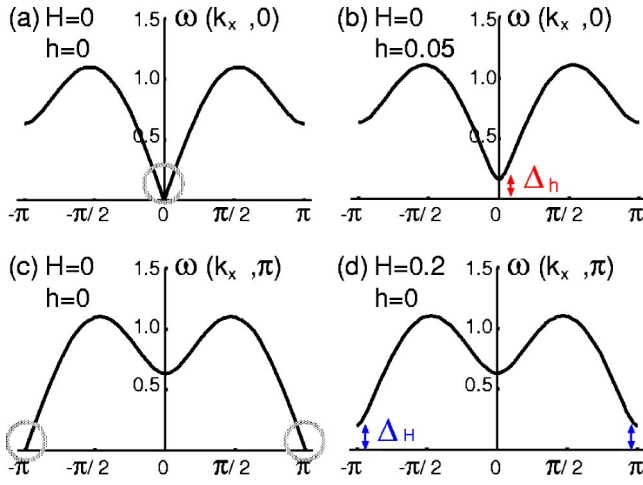


FIG. 7. Magnon dispersions of the SSB phase in the 2D competitive case for $(S, J, J_\perp) = (1/2, 1, 0.1)$ and $a_x = a_y = 1$. The gray circles represent the gapless points.

$$\sin \phi_{cl} = \frac{h}{4S(J_\perp + J'_\perp)}.$$

For the resulting quadratic Hamiltonian \hat{H}_{HP} , we perform a Fourier transformation (FT) $c_{i,j,k}^\dagger = N^{-d/2} \sum_{\vec{k}} e^{i\vec{k} \cdot \vec{r}} c_{\vec{k}}^\dagger$, where N is the linear system size, d is the dimension of the system, k_α ($|k_\alpha| < \pi/a_\alpha$) and a_α are, respectively, the wave number and the lattice constant for the α direction. A four-mode Bogoliubov transformation (BT),²⁶ which mixes $c_{\vec{k}}, c_{-\vec{k}}, c_{\vec{k}-\vec{\pi}}, c_{-\vec{k}-\vec{\pi}}$ and their Hermitian conjugates ($\vec{\pi} \equiv (0, \pi/a_y, \pi/a_z)$), leads to the diagonalized form

$$\hat{H}_{HP} = \sum_{\vec{k}} \omega(\vec{k}) c_{\vec{k}}^\dagger c_{\vec{k}} + \text{const} \quad (16)$$

with a single band in the first Brillouin zone, where $c_{\vec{k}}$ is the magnon annihilation operator and the k_x direction corresponds to the strongly AF one. The explicit results on the dispersion $\omega(\vec{k})$ are lengthy and thus are given in the Appendix. Here we discuss physical implications of our results.

First, the obtained dispersion satisfies $\omega(\vec{k}) \geq 0$ for all values of parameters. This implies that the SSB phase, which appears as the classical ground state, is stable against quantum fluctuations, at least in the lowest order of $1/S$. Some representatives of the dispersion are shown in Fig. 7. At zero field ($H = h = 0$), there are two gapless points $\vec{k}_h = (0, 0, 0)$ and $\vec{k}_H = (\pi/a_x, \pi/a_y, \pi/a_z)$, with linear dispersions in the neighborhoods. Let us define $\Delta_h = \omega(\vec{k}_h)$ and $\Delta_H = \omega(\vec{k}_H)$. Since our results in Section 1 of the Appendix indicates that Δ_h (Δ_H) is nonvanishing only when $h \neq 0$ ($H \neq 0$), we call it as h (H)-induced gap. The true excitation gap, namely, the minimum excitation energy, is given by $\Delta = \min(\Delta_h, \Delta_H)$. Thus the gap Δ vanishes exactly as long as either h or H remains zero. This is contrasting to the $S = 1/2$ 1D HAF model, where the staggered field alone induces the gap.²⁷ The gapless excitations are identified as Nambu-Goldstone (NG) modes. Indeed, when either H or h is zero, the Hamil-

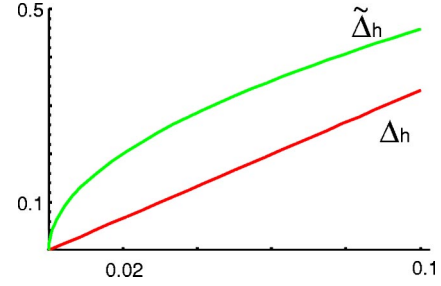


FIG. 8. Δ_h and $\tilde{\Delta}_h$ in the 2D case for $(S, J, J_\perp, H) = (1/2, 1, 0.1, 0)$. In the present case where $H = 0$, the gaps have simple forms: $\Delta_h = (1 + J/J_\perp)^{1/2} h$ and $\tilde{\Delta}_h = [1 + h/(4SJ)]^{1/2} \sqrt{4SJ} h$ (see the Appendix).

tonian has a continuous $U(1)$ symmetry, which is broken spontaneously in the SSB phase.

In the noncompetitive case, the magnon dispersion relation $\tilde{\omega}(\vec{k})$ is given in Eq. (A20). Now the staggered field alone can open the gap, because the ground state does not break any continuous symmetry spontaneously. On the other hand, the system remains gapless at $\vec{k} = 0$ due to the NG mechanism if $h = 0$ and H is not too large. The h -induced gap is thus defined as $\tilde{\Delta}_h = \tilde{\omega}(\vec{k} = \vec{0})$.

While the h -induced gap is defined for both cases, there is a characteristic difference in the h dependence of the gaps. In the limit of small h , $\tilde{\Delta}_h \sim h^{1/2}$ for the noncompetitive case, but $\Delta_h \sim h$ for the competitive case. In other words, one can say that the h -induced gap in the competitive case opens more slowly than in the noncompetitive case. This is naturally understood because the competition between J_\perp (or J'_\perp) and h weakens the effect of the external symmetry breaking by h . It also implies that the ground state is more stable in the noncompetitive case, against quantum and thermal fluctuations. The opening gaps are drawn in Fig. 8. On the other hand, in the limit of small H , $\Delta_H \sim H$. Similarly to the case of Δ_h , this may be interpreted as a result of the competition between the uniform field and the AF couplings.

We expect the spin-wave theory for the gaps to be qualitatively correct even for $S = 1/2$. As discussed in Sec. 2 of the Appendix, the spin-wave dispersion of the symmetric phase can be obtained by the replacement $(|J_\perp|, |J'_\perp|) \rightarrow (-J_\perp, -J'_\perp)$ in the dispersion of the noncompetitive case.

Finally let us discuss the relation of the present results to the spin-wave theory in the 1D model ($J_\perp = J'_\perp = 0$) with the staggered field h discussed in Ref. 5. The spin-wave dispersion $\tilde{\omega}(\vec{k})$ for the noncompetitive case does approach smoothly to the 1D dispersion [Eq. (3.11) in Ref. 5], when $J_\perp, J'_\perp \rightarrow 0$. On the other hand, the dispersion $\omega(\vec{k})$ for the competitive case apparently does not reduce to the 1D one in the limit of $J_\perp, J'_\perp \rightarrow 0$. This is because $\omega(\vec{k})$ is the dispersion of the magnon excitation in the SSB phase, which is absent in the 1D model. In fact, for any finite h , the SSB phase is realized [and hence $\omega(\vec{k})$ is applicable] only when J_\perp and J'_\perp are above the critical values. Thus by decreasing J_\perp (J'_\perp) at a fixed h , the system undergoes a phase transition into the symmetric phase. At the transition the dispersion

should also change drastically. In the symmetric phase, similarly to the noncompetitive case, the dispersion does approach continuously to the 1D dispersion.

IV. CHAIN MEAN-FIELD THEORY APPROACH

In this section, we reconstruct the phase diagram of our model using chain mean-field theory (CMFT). In the CMFT, weak couplings among the chains are treated with a MFT, and the resulting effective 1D problem is analyzed as precisely as possible. If the 1D problem can be treated exactly, the CMFT is expected to be much more reliable when the one dimensionality is strong enough as in the case of Cu-benzoate, since it includes the fluctuations in the strongly coupled direction correctly. The usefulness of the CMFT has been demonstrated in several applications.^{23,24,28}

In Sec. IV A, we discuss how the CMFT determines the phase transition for our model (3). Section IV B is a brief overview of susceptibilities of the $S=1/2$ HAF chain which are necessary to the CMFT. In Sec. IV C, we present the CMFT phase diagrams and compare them to the MFT ones.

A. CMFT for our model

Let us derive the effective 1D model for our system (3), within the CMFT.

In the competitive case, we consider the symmetric phase side for convenience. The mean-field procedure for the weak interchain couplings replaces them with the effective external fields. Thus the resulting Hamiltonian is

$$\begin{aligned} \hat{H} &\rightarrow \sum_{j,k} \hat{H}_{j,k} + N^d (J_{\perp} + J'_{\perp}) (m_y^2 - m_x^2 - m_z^2), \\ \hat{H}_{j,k} &= \sum_i J \tilde{S}_{i,j,k} \cdot \tilde{S}_{i+1,j,k} - (-1)^{j+k} [h' + 2(J_{\perp} + J'_{\perp})m_y] \\ &\quad \times (-1)^i S_{i,j,k}^y - [h - 2(J_{\perp} + J'_{\perp})m_x] (-1)^i S_{i,j,k}^x \\ &\quad - [H - 2(J_{\perp} + J'_{\perp})m_z] S_{i,j,k}^z, \end{aligned} \quad (17)$$

where we introduced an infinitesimal staggered field $(-1)^{j+k}h'$ parallel to the order parameter. The CMFT requires that the mean fields $m_{x,y,z}$ are equivalent to the corresponding moments of the effective chain $\hat{H}_{j,k}$. It has the two effective staggered fields $h_x \equiv h - 2(J_{\perp} + J'_{\perp})m_x$ and $h_y \equiv h' + 2(J_{\perp} + J'_{\perp})m_y$ as well as the effective uniform field $H_z \equiv H - 2(J_{\perp} + J'_{\perp})m_z$. Clearly it is sufficient to consider one chain where $j+k$ is even, and we represent it as \hat{H}_{1D} . Within the linear-response theory, the moment $|\langle S_i^y \rangle|$, in which $\langle \dots \rangle$ stands for the mean value of \hat{H}_{1D} , can be approximated by $\chi_y^{\text{1D}}(H_z, h_x, 0)h_y$ where the staggered susceptibility is defined as $\chi_y^{\text{1D}}(H_z, h_x, h_y) \equiv \partial |\langle S_i^y \rangle| / \partial h_y$. Therefore the above requirement leads to $m_y = \chi_y^{\text{1D}} h_y$ which is transformed to

$$m_y = \frac{\chi_y^{\text{1D}}}{1 - 2(J_{\perp} + J'_{\perp})\chi_y^{\text{1D}}} h'. \quad (18)$$

Similarly m_x and m_z can be determined by the CMFT as well. The critical condition of our model is

$$1 - 2(J_{\perp} + J'_{\perp})\chi_y^{\text{1D}}(H_z, h_x, 0) = 0. \quad (19)$$

At this point, one sees that the original 3D or 2D susceptibilities and moments can be described by those of the effective chain.

The staggered field in \hat{H}_{1D} has both x and y components: h_x and h_y . By the infinitesimal rotation $R_z(\delta)$ about z axis by angle δ , where $\sin \delta = -[h_y^2/(h_y^2 + h_x^2)]^{1/2}$, the effective Hamiltonian is simplified as

$$\hat{H}'_{1D} = \sum_i J \tilde{S}'_i \cdot \tilde{S}'_{i+1} - H_z S_i'^z - h'_x (-1)^i S_i'^x \quad (20)$$

with the one-component staggered field $h'_x = h_x / \cos \delta$. In order to obtain an alternative formula determining m_y instead of Eq. (18), we focus on the relation

$$\langle S_i'^x \rangle' = \cos \delta \langle S_i^x \rangle - \sin \delta \langle S_i^y \rangle = (-1)^i (\cos \delta m_x - \sin \delta m_y), \quad (21)$$

where $\langle \dots \rangle'$ represents the expectation value of \hat{H}'_{1D} and the second equality is caused by the self-consistency of the CMFT. Here we define the susceptibilities of the HAF chain (20) as $\chi_u^{\text{1D}}(T, H_z, h'_x) \equiv \partial m'_u / \partial H_z$ and $\chi_s^{\text{1D}}(T, H_z, h'_x) \equiv \partial m'_s / \partial h'_x$ where $m'_{x,z} = |\langle S_i^{x,z} \rangle'|$. Within the linear-response theory Eq. (21) is reduced to

$$\chi_s^{\text{1D}}(T, H_z, h'_x) h'_x = \cos \delta m_x - \sin \delta m_y. \quad (22)$$

Let us recall that δ is defined by m_x and m_y , and that $m_{x,z}$ are determined by the CMFT. Consequently, m_y can be determined as a solution to Eq. (22). The condition that m_y diverges would determine the phase transition.

B. Susceptibilities of $S=1/2$ AF chains

In order to solve Eq. (19) or (22) in terms of m_y , we need the explicit forms of the susceptibilities: χ_u^{1D} and χ_s^{1D} . Here we briefly summarize the known results^{5,29-31} on these quantities, obtained by the bosonization technique.

In the absence of the staggered field h'_x , the low-energy effective theory of the Heisenberg chain (20) is given by a free boson field theory, and the uniform susceptibility at zero temperature is obtained as

$$\chi_u^{\text{1D}}(T, H, 0) \approx \frac{a}{(2\pi)^2 R(H)^2 v(H)}, \quad (23)$$

where $H_z = H$, and R and v , respectively, are the compactification radius of the effective boson field theory²⁹⁻³³ and the spin-wave velocity. The exact values $v(H)$ and $R(H)$ as functions of the uniform field H are given by a solution of a set of the Bethe ansatz integral equations.³⁴ In the case of $H=0$, they are explicitly given as

$$v = \pi J a / 2, \quad R = 1 / \sqrt{2\pi}. \quad (24)$$

For a small uniform field $H_z = H (\ll J)$, the asymptotic behavior of the radius R follows⁵

$$2\pi R^2 \approx 1 - \frac{1}{2\ln(J/H)}. \quad (25)$$

The logarithmic temperature correction due to the marginal operator of the HAF chain is discussed in Ref. 35. Although the transverse staggered field h'_x induces a gap, it is expected

to have little effect^{1,5} on the uniform susceptibility χ_u^{1D} if h'_x is small enough.

Next we turn to the staggered susceptibility χ_s^{1D} . In the case $J \gg h'_x, k_B T$, the low-energy effective theory of the Hamiltonian (20) is given by a quantum sine-Gordon field theory. Using the exact solutions of the HAF chain, the scaling arguments and Lukyanov-Zamolodchikov prediction,^{36,37} the staggered susceptibility χ_s^{1D} for small $H_z = H$ and $h'_x = h$ at $T = 0$ ^{1,5} is given as

$$\chi_s^{1D} \approx \begin{cases} D [2(1 - 2\pi R^2)]^{-1/3} \frac{\pi R^2}{2 - \pi R^2} \left(\frac{J}{H}\right)^{-2(1 - 2\pi R^2)/3} \left(\frac{h}{J}\right)^{\pi R^2/(2 - \pi R^2)} h^{-1} & (H \gg h) \\ D e^{-1/3} \frac{1}{3} \left[\ln\left(\frac{J}{H}\right)\right]^{1/3} \left(\frac{h}{J}\right)^{1/3} h^{-1} & (J \gg H \gg h) \\ D \frac{2^{1/3}}{3^{4/3}} \left[\frac{h}{J} \ln\left(\frac{J}{h}\right)\right]^{1/3} h^{-1} & (H = 0), \end{cases} \quad (26)$$

where the radius R is that of the model without the staggered field, and $D \equiv 0.3868 \dots$. The first formula is actually valid for $H \leq 2J$ (below saturation field), but the second is only so for $H \ll J$. These formulas are correct in $k_B T \ll h \ll J$. (More precisely, within $k_B T \ll \Delta_h \ll J$ where Δ_h is the h -induced gap in the HAF chain.⁵)

In the intermediate temperature regime $h, H \ll k_B T \ll J$, where the temperature is larger than the induced gap, the staggered susceptibility may be approximated by that for zero staggered field⁵ as

$$\chi_s^{1D}(k_B T \gg h) \approx D \frac{[\ln(J/k_B T)]^{1/2}}{k_B T}, \quad (27)$$

where $D \equiv 0.2779 \dots$.

C. Phase diagrams in CMFT

Employing the results of Secs. IV A and IV B, we study the phase diagrams, in particular for the competitive case, within the CMFT. Unfortunately, it can be applied only to several limited regions in the parameter space, where the susceptibilities of the 1D model are obtained exactly.

First, let us consider the region near $(k_B T_c, 0, 0)$. In the zero-field case, the effective model \hat{H}_{1D} has only an infinitesimal staggered mean field h_y as long as it is in the symmetric phase. Therefore the formula (27) can give the self-consistent value of m_y , and Eq. (19) is the critical condition which serves the critical temperature:

$$\begin{aligned} k_B T_c &= 2D(J_\perp + J'_\perp) \left[\ln\left(\frac{J}{k_B T_c}\right) \right]^{1/2} \\ &\approx 2D(J_\perp + J'_\perp) \left[\ln\left(\frac{J}{2D(J_\perp + J'_\perp)}\right) \right]^{1/2}, \end{aligned} \quad (28)$$

which is reasonable when $k_B T_c, (J_\perp + J'_\perp) \ll J$ and agrees with the result of Ref. 24. Equation (28) is also stable against a small staggered field h , because χ_s^{1D} is independent of h in Eq. (27). These results are also valid for the noncompetitive case, with the replacement $J_\perp + J'_\perp \rightarrow |J_\perp| + |J'_\perp|$. Figure 9 represents the comparison between the CMFT result (28) and the mean-field prediction: $k_B T_c = (J + J_\perp + J'_\perp)/2$.

Next we investigate the neighborhood of $(0, 0, h_c)$. In this case ($H = 0$), \hat{H}_{1D} has two staggered fields. Therefore through the rotation of Sec. IV B, the order parameter m_y can be fixed by Eq. (22). Inserting the third formula of Eq. (26) into Eq. (22), and performing the Taylor expansion of Eq. (26) around $h_y = 0$, we obtain the linear-response relation

$$m_y = \frac{\left\{ \frac{2}{3} - \frac{1}{6} [\ln(J/h_x)]^{-1} \right\} m_x}{h - \frac{1}{3} \{ 10(J_\perp + J'_\perp) - [\ln(J/h_x)]^{-1} \} m_x} h'. \quad (29)$$

Therefore the critical condition can be written as

$$m_x \approx \frac{3h_c}{10(J_\perp + J'_\perp)}, \quad (30)$$

where we assumed $h_c, (J_\perp + J'_\perp) \ll J$. On the other hand, m_x should be fixed from the self-consistency of the CMFT as well. At $T = 0$, it leads to

$$m_x = \frac{\chi_s^{1D}(0, 0, h - 2(J_\perp + J'_\perp)m_x)}{1 + 2(J_\perp + J'_\perp)\chi_s^{1D}(0, 0, h - 2(J_\perp + J'_\perp)m_x)} h. \quad (31)$$

Combining Eqs. (30) and (31), we obtain the critical staggered field

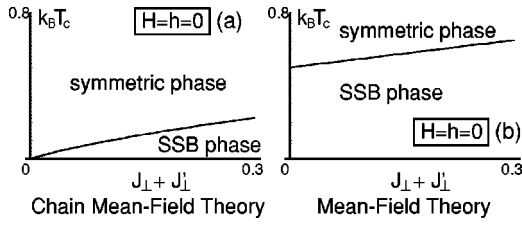


FIG. 9. $(k_B T_c, J_\perp + J'_\perp)$ in the competitive case for $J=1$. (a) and (b) are, respectively, predicted within the CMFT and the MFT. It is confirmed that the SSB areas of the CMFT are considerably smaller than the MFT.

$$h_c = D' \left[\frac{J_\perp + J'_\perp}{J} \ln \left(\frac{5J}{2h_c} \right) \right]^{1/2} 2(J_\perp + J'_\perp)$$

$$\approx D' \left\{ \frac{J_\perp + J'_\perp}{J} \ln \left[\frac{5}{4D'} \left(\frac{J}{J_\perp + J'_\perp} \right)^{1/2} \right] \right\}^{1/2} 2(J_\perp + J'_\perp), \quad (32)$$

where we kept only the leading order of $(J_\perp + J'_\perp)/J$ and $D' \equiv (2 \times 10^2 D^3 3^{-7})^{1/2} \approx 7.27 \dots \times 10^{-2}$. This is valid if $h_c, (J_\perp + J'_\perp) \ll J$, and is compared to the MFT result $h_c = 2(J_\perp + J'_\perp)$ extracted from Eq. (8) in Fig. 10. The CMFT correction to the MFT is found as a significant multiplicative factor $D'[\dots]^{1/2}$.

We consider furthermore the critical line in the $T=0$ plane in the limit of $h_c \ll H_c \ll J$. In the symmetric phase near this line, the effective model \hat{H}_{1D} has all three kinds of the external fields. Hence m_x and m_z must be determined concurrently by the CMFT scheme. However, in the present case $h_c \ll H_c$, m_x may be estimated independently by taking an approximation $\chi_u^{1D}(0, H, h) \sim \chi_u^{1D}(0, H, 0)$ which was given in Eq. (23). From this approximation, m_z is also fixed as

$$m_z \approx \frac{H}{\pi^2 J \{1 - [\ln(J/H)]^{-1}\} + 2(J_\perp + J'_\perp)}, \quad (33)$$

which is justified in $H, (J_\perp + J'_\perp) \ll J$. In the sufficiently small field case, $J \gg H (\gg h)$, the logarithmic part can be dropped as well. From the second of Eqs. (26) and Eqs. (30), (31), and (33), we obtain the critical line in $T=0$,

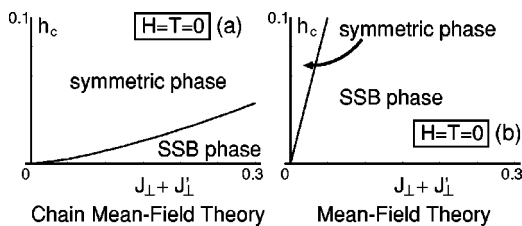


FIG. 10. $(h_c, J_\perp + J'_\perp)$ in the competitive case for $J=1$. (a) and (b) are, respectively, predicted within the CMFT and the MFT. Similarly to Fig. 9, the narrowing of the SSB areas occurs.

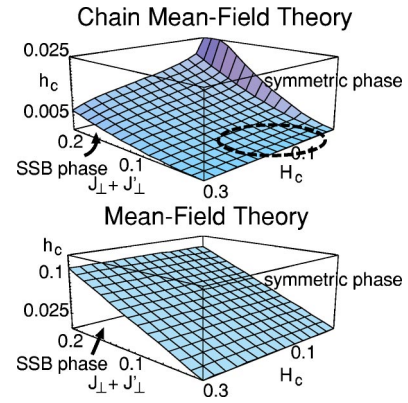


FIG. 11. Critical surface (h_c, H_c) in the competitive case for $(J, T) = (1, 0)$ obtained with the CMFT (34) (upper panel) and the MFT (8) (lower panel). In the whole region of the CMFT panel, the critical region surrounded by the dashed ring ($h_c \ll H_c \ll J$) is greatly reliable.

$$h_c = D'' \left\{ \frac{J_\perp + J'_\perp}{J} \left[\ln \left(\frac{\pi^2 J [1 - [\ln(J/H_c)]^{-1}] + 2(J_\perp + J'_\perp)}{\pi^2 H_c} \right) + [\ln(J/H_c)]^{-1} + \dots \right] \right\}^{1/2} 2(J_\perp + J'_\perp), \quad (34)$$

where $D'' \equiv (10^2 D^3 e^{-1} 3^{-6})^{1/2} \approx 5.40 \dots \times 10^{-2}$. This condition is presumably suitable for $k_B T_c \ll h_c \ll H_c \ll J$. Thus, in order to obtain a more precise condition, it is necessary to adopt the first formula (26) and the exact values of R and v . Figure 11 exhibits the comparison between this line and the mean-field prediction.

Finally, we consider the point $(0, H_c, 0)$, where \hat{H}_{1D} has only the uniform field $H_z = H_c - 2(J_\perp + J'_\perp)m_z$ except for the infinitesimal field h_y . It has been known from Bethe ansatz that the magnetization saturates at the point $H_z = 2J$ at $T=0$ in the HAF chain having only the field H_z . The transition point between the SSB and symmetric phase in this case should be identified with the saturation of the uniform magnetization. Hence, within the CMFT, the critical uniform field is given as

$$H_c = 2J + (J_\perp + J'_\perp). \quad (35)$$

The substitution $J_\perp + J'_\perp \rightarrow -(|J_\perp| + |J'_\perp|)$ gives the critical field of the AF-paramagnetic transition in the noncompetitive case.

From these results, we can compare the CMFT and the MFT phase diagrams. The comparison for the competitive case is summarized in Fig. 12. In the case of weak interchain couplings ($J \gg J_\perp, J'_\perp$), the SSB phase of the CMFT is much smaller than one of the MFT. Especially there is a significant narrowing in $k_B T$ and h directions. As seen from Eq. (18), this is because the phase transition in the CMFT framework is driven by the divergence of the susceptibility (in the present case, χ_s^{1D}) in the effective chain, while temperature and the field h_x (or m_x) suppress the divergence. On the other hand, the reduction of the critical uniform field H_c is small in the weakly coupled case. This is because the uni-

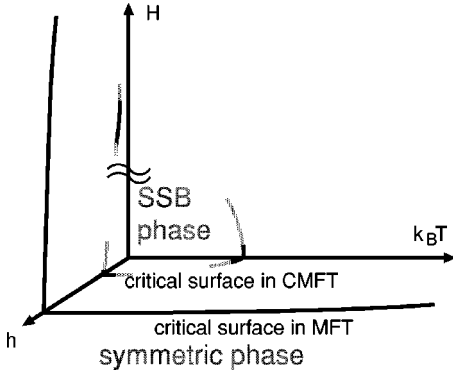


FIG. 12. Schematic phase diagrams of the CMFT and the MFT in the competitive case.

form field competes with the intrachain AF interaction as well as with the interchain interactions.

Finally we review the validity of the two theories. Since the strong one dimensionality is the basis of the CMFT procedure, it is expected that the CMFT is more reliable in the limit of $J \gg J_{\perp}, J'_{\perp}$. On the other hand, when J_{\perp} and J'_{\perp} are comparable to J , the special treatment of only one direction is unjustified. Therefore the MFT, which treats all couplings equally, is more reasonable for $J \sim J_{\perp}, J'_{\perp}$.

V. SUMMARY AND DISCUSSION

We considered the effects of the staggered field h in an $S=1/2$ Heisenberg antiferromagnet (3) in two or three dimensions. The system behaves quite differently depending on whether the staggered field and the interchain couplings are competitive or not. In the competitive case, the appearance of a characteristic ordered (SSB) phase is predicted by the MFT. The SSB phase breaks the translational symmetry of the weakly coupled direction, and therefore it is peculiar to high-dimensional systems. We also applied the CMFT to the model (3), and predicted that the region of the SSB phase becomes narrow in the CMFT scheme. The MFT and the CMFT are valid, respectively, in $J \sim J_{\perp}, J'_{\perp}$ and in $J \gg J_{\perp}, J'_{\perp}$. The crossover behavior between these two regions cannot be described by the mean-field type approach.³⁸⁻⁴⁰ It would require a more precise treatment of fluctuations.

Moreover we studied spin-wave theory in both the competitive and noncompetitive cases at $T=0$. When the uniform field H is nonvanishing, the h -induced gap opens as $\Delta_h \sim h$ in the SSB phase, while $\tilde{\Delta}_h \sim h^{1/2}$ in the AF phase of the noncompetitive case. This difference reflects the partial cancellation of the staggered field effect due to the competitive interchain interaction in the SSB phase. The spin-wave dispersion in the SSB phase remains gapless due to NG mechanism even under a nonvanishing h . This is in contrast to the case of the 1D model.

Finally we comment on a few recent reports related to our study. In $\text{BaCu}_2\text{Si}_2\text{O}_7$ reported in Ref. 41, both the staggered field and the interchain interactions are expected, as in our models. However, the effect of the exchange anisotropies, which is ignored in the present paper, is argued to be responsible for the observed two spin-flip transitions. Extending

the present work to such a system would be an interesting problem in the future. Furthermore, in $\text{BaCu}_2(\text{Si}_{1-x}\text{Ge}_x)_2\text{O}_7$,²² the sign of the interchain interaction seems to depend on the doping parameter x . Thus, it could provide a realization of the competitive and noncompetitive cases.

Wang *et al.*² investigated an $S=1/2$ AF ladder system with a staggered field. They argue that the competition between the staggered field and the rung interaction brings a quantum criticality. It might be interesting to compare our analysis on the higher-dimensional system with theirs.

ACKNOWLEDGMENTS

We thank Collin Broholm, Dan Reich, and Hidekazu Tanaka for useful comments. This work was partially supported by Grant-in-Aid by MEXT of Japan.

APPENDIX: DETAILS OF SPIN-WAVE RESULTS IN SEC. III

Here we supplement the spin-wave results omitted in Sec. III.

1. The competitive case

We write down the details of the competitive case. After the FT of the boson operator $c_{i,j,k}$, the spin-wave Hamiltonian can be expressed as the following matrix form:

$$\hat{H}_{\text{HP}} = \sum_{\vec{k}} \begin{pmatrix} c_{\vec{k}}^{\dagger T} & c_{\vec{k}}^T \end{pmatrix} \begin{pmatrix} \xi_{\vec{k}} & \eta_{\vec{k}} \\ \eta_{\vec{k}}^* & \xi_{\vec{k}}^* \end{pmatrix} \begin{pmatrix} c_{\vec{k}} \\ c_{\vec{k}}^{\dagger} \end{pmatrix} - 4E_1(\vec{k}) + E_{\text{gs}}^{\text{cl}}, \quad (\text{A1})$$

where * and T , respectively, stand for the complex conjugate of each matrix component and the transpose of matrices, and the 4×4 matrices $\xi_{\vec{k}}$, $\eta_{\vec{k}}$ and the column four-vector $C_{\vec{k}}$ are given as

$$\xi_{\vec{k}} = \begin{pmatrix} E_1(\vec{k}) & 0 & 0 & iE_4(k_{y,z}) \\ 0 & E_1(\vec{k}) & iE_4(k_{y,z}) & 0 \\ 0 & -iE_4(k_{y,z}) & F_1(\vec{k}) & 0 \\ -iE_4(k_{y,z}) & 0 & 0 & F_1(\vec{k}) \end{pmatrix},$$

$$\eta_{\vec{k}} = \begin{pmatrix} 0 & E_2(\vec{k}) & 0 & iE_3(k_x) \\ E_2(\vec{k}) & 0 & iE_3(k_x) & 0 \\ 0 & iE_3(k_x) & 0 & F_2(\vec{k}) \\ iE_3(k_x) & 0 & F_2(\vec{k}) & 0 \end{pmatrix},$$

$$C_{\vec{k}} = (c_{\vec{k}} \ c_{-\vec{k}} \ c_{\vec{k}-\vec{\pi}} \ c_{-\vec{k}-\vec{\pi}})^T. \quad (\text{A2})$$

Here $E_{1,2,3,4}$ are defined as

$$\begin{aligned}
 E_1(\vec{k}) = & [2SJ(1 - 2 \sin^2 \theta_{\text{cl}} \cos^2 \phi_{\text{cl}}) + 2S(J_{\perp} + J'_{\perp}) \\
 & \times (2 \cos^2 \theta_{\text{cl}} \cos^2 \phi_{\text{cl}} - 1) \\
 & - 2SJ \sin^2 \theta_{\text{cl}} \cos^2 \phi_{\text{cl}} \cos k_x a_x \\
 & + 2S(\cos^2 \theta_{\text{cl}}(1 + \sin^2 \phi_{\text{cl}}) - 1)(J_{\perp} \cos k_y a_y \\
 & + J'_{\perp} \cos k_z a_z) + H \sin \theta_{\text{cl}} \cos \phi_{\text{cl}} + h \sin \phi_{\text{cl}}]/8,
 \end{aligned}$$

$$\begin{aligned}
 E_2(\vec{k}) = & [SJ(\cos^2 \theta_{\text{cl}} - \sin^2 \theta_{\text{cl}} \sin^2 \phi_{\text{cl}}) \cos k_x a_x \\
 & + S \cos^2 \theta_{\text{cl}} \cos^2 \phi_{\text{cl}} (J_{\perp} \cos k_y a_y + J'_{\perp} \cos k_z a_z)]/4,
 \end{aligned}$$

$$E_3(k_x) = -SJ \sin 2 \theta_{\text{cl}} \sin \phi_{\text{cl}} \cos k_x a_x / 4,$$

$$E_4(k_{y,z}) = S \sin 2 \theta_{\text{cl}} \sin \phi_{\text{cl}} (J_{\perp} \cos k_y a_y + J'_{\perp} \cos k_z a_z) / 4, \quad (\text{A3})$$

and $F_{1,2}(\vec{k}) = E_{1,2}(\vec{k} - \vec{\pi})$. Thus $\xi_{\vec{k}}$ is Hermitian and $\eta_{\vec{k}}$ is symmetric. Let us suppose that a four-mode BT

$$\begin{pmatrix} \tilde{\mathcal{C}}_{\vec{k}} \\ \tilde{\mathcal{C}}_{\vec{k}}^{\dagger} \end{pmatrix} = M_{\text{BT}}(\vec{k}) \begin{pmatrix} \mathcal{C}_{\vec{k}} \\ \mathcal{C}_{\vec{k}}^{\dagger} \end{pmatrix}, \quad (\text{A4})$$

where $\tilde{\mathcal{C}}_{\vec{k}} = (\tilde{c}_{\vec{k}}, \tilde{c}_{-\vec{k}}, \tilde{c}_{\vec{k}-\vec{\pi}}, \tilde{c}_{-\vec{k}-\vec{\pi}})^T$ is a set of new boson (magnon) operators and $M_{\text{BT}}(\vec{k})$ is an 8×8 matrix, diagonalizes the Hamiltonian as follows:

$$\hat{H}_{\text{HP}} = \sum_{\vec{k}} \begin{pmatrix} \tilde{\mathcal{C}}_{\vec{k}}^{\dagger} & \tilde{\mathcal{C}}_{\vec{k}}^{\dagger} \end{pmatrix} \begin{pmatrix} \Omega_{\vec{k}} & 0 \\ 0 & \Omega_{\vec{k}} \end{pmatrix} \begin{pmatrix} \tilde{\mathcal{C}}_{\vec{k}} \\ \tilde{\mathcal{C}}_{\vec{k}}^{\dagger} \end{pmatrix} - 4E_1(\vec{k}) + E_{\text{gs}}^{\text{cl}}, \quad (\text{A5})$$

where $\Omega_{\vec{k}} = \text{diag}[\omega_1(\vec{k}), \omega_2(\vec{k}), \omega_3(\vec{k}), \omega_4(\vec{k})]$. According to Ref. 26, determining $\Omega_{\vec{k}}$ and $M_{\text{BT}}(\vec{k})$ is equivalent to solving an eigenvalue problem

$$\begin{pmatrix} \xi_{\vec{k}} & -\eta_{\vec{k}} \\ \eta_{\vec{k}}^* & -\xi_{\vec{k}}^* \end{pmatrix} M_{\text{BT}}^{\dagger} = M_{\text{BT}}^{\dagger} \begin{pmatrix} \Omega_{\vec{k}} & 0 \\ 0 & -\Omega_{\vec{k}} \end{pmatrix}. \quad (\text{A6})$$

The eight eigenvalues $\pm \omega_j(\vec{k})$ ($j=1,2,3,4$) are given by $\pm \lambda_l$ ($l=1,2,3,4$), where

$$\begin{aligned}
 \lambda_1(\vec{k}) = & [1/2 G_{\vec{k}} - 1/2(G_{\vec{k}}^2 - 4G_{\vec{k}}^{\pm})^{1/2}]^{1/2}, \\
 \lambda_2(\vec{k}) = & [1/2 G_{\vec{k}} - 1/2(G_{\vec{k}}^2 - 4G_{\vec{k}}^{\mp})^{1/2}]^{1/2}, \\
 \lambda_3(\vec{k}) = & [1/2 G_{\vec{k}} + 1/2(G_{\vec{k}}^2 - 4G_{\vec{k}}^{\pm})^{1/2}]^{1/2}, \\
 \lambda_4(\vec{k}) = & [1/2 G_{\vec{k}} + 1/2(G_{\vec{k}}^2 - 4G_{\vec{k}}^{\mp})^{1/2}]^{1/2}, \quad (\text{A7})
 \end{aligned}$$

and $G_{\vec{k}}$ and $G_{\vec{k}}^{\pm}$ are defined as

$$\begin{aligned}
 G_{\vec{k}} = & E_1^2 - E_2^2 + F_1^2 - F_2^2 - 2E_3^2 + 2E_4^2, \\
 G_{\vec{k}}^{\pm} = & (E_3^2 - E_4^2)^2 + (E_1^2 - E_2^2)(F_1^2 - F_2^2) - 2(E_1 F_1 - E_2 F_2) \\
 & \times (E_3^2 + E_4^2) \mp 4(E_1 F_2 - E_2 F_1) E_3 E_4. \quad (\text{A8})
 \end{aligned}$$

The physical dispersion $\omega(\vec{k})$ is given by either $4[\lambda_1(\vec{k}) + \lambda_2(\vec{k})]$ or $4[\lambda_3(\vec{k}) + \lambda_4(\vec{k})]$, depending on the value of \vec{k} . In the vicinity of the point $\vec{k} = \vec{k}_h$ (\vec{k}_H), which is the gapless point when $h=0$ ($H=0$), we find

$$\omega(\vec{k}) = 4[\lambda_1(\vec{k}) + \lambda_2(\vec{k})]. \quad (\text{A9})$$

If only one of the external fields (H or h) is nonvanishing, the result is considerably simplified because we have $E_3 = E_4 = 0$. The spin-wave Hamiltonian can be actually diagonalized by a simpler two-mode BT which is the same type as we need in the noncompetitive case in the following subsection. The resulting magnon dispersion is

$$\begin{aligned}
 \omega(\vec{k}) = & \{ [2SJ(1 - 2 \sin^2 \theta_{\text{cl}} \cos^2 \phi_{\text{cl}}) + 2S(J_{\perp} + J'_{\perp}) \\
 & \times (2 \cos^2 \theta_{\text{cl}} \cos^2 \phi_{\text{cl}} - 1) \\
 & - 2SJ \sin^2 \theta_{\text{cl}} \cos^2 \phi_{\text{cl}} \cos k_x a_x + 2S(\cos^2 \theta_{\text{cl}}(1 \\
 & + \sin^2 \phi_{\text{cl}}) - 1)(J_{\perp} \cos k_y a_y + J'_{\perp} \cos k_z a_z) + \Sigma]^2 \\
 & - [2SJ(\cos^2 \theta_{\text{cl}} - \sin^2 \theta_{\text{cl}} \sin^2 \phi_{\text{cl}}) \cos k_x a_x \\
 & + 2S \cos^2 \theta_{\text{cl}} \cos^2 \phi_{\text{cl}} (J_{\perp} \cos k_y a_y \\
 & + J'_{\perp} \cos k_z a_z)]^2 \}^{1/2}, \quad (\text{A10})
 \end{aligned}$$

where $\Sigma = H \sin \theta_{\text{cl}} \cos \phi_{\text{cl}}$ when $h=0$, and $\Sigma = h \sin \phi_{\text{cl}}$ when $H=0$. Of course, in these special cases, Eq. (A9) reduces to Eq. (A10) near $\vec{k} = \vec{k}_h$ or \vec{k}_H .

From the dispersion (A9), let us estimate how Δ_h (Δ_H) grows when a small h (H) is applied. To estimate Δ_h , it is sufficient to know the coefficients of Taylor expansion of $E_{1,2,3,4}(\vec{k} = \vec{0})$, $G_{\vec{k}=\vec{0}}$, and $G_{\vec{k}=\vec{0}}^{\pm}$ around $h=0$. As a result, in the limit of small h , the gap behaves as

$$\begin{aligned}
 \Delta_h \approx & 2S(J + J_{\perp} + J'_{\perp})^{1/2} (J_{\perp} + J'_{\perp})^{1/2} (1 - \tilde{H}^2)^{1/2} \\
 & \times \left(1 - \tilde{H}^2 + \frac{J_{\perp} + J'_{\perp}}{J} \tilde{H}^2 \right)^{-1/2} \\
 & \times \left[\left(1 - 4\tilde{H}^2 - \frac{(J - J_{\perp} - J'_{\perp})^2}{J(J_{\perp} + J'_{\perp})} \tilde{H}^4 \right)^{1/2} \right. \\
 & \left. + \left(1 - \frac{(J - J_{\perp} - J'_{\perp})^2}{J(J_{\perp} + J'_{\perp})} \tilde{H}^4 \right)^{1/2} \right] \tilde{h} + \dots, \quad (\text{A11})
 \end{aligned}$$

where $\tilde{H} = H/[4S(J + J_{\perp} + J'_{\perp})]$ and $\tilde{h} = h/[4S(J_{\perp} + J'_{\perp})]$. At $H=0$, Eq. (A11) is reduced to the exact result $\Delta_h = [1 + J/(J_{\perp} + J'_{\perp})]^{1/2} h$ which is derived from Eq. (A10) and is drawn in Fig. 8. Similarly to Δ_h , Δ_H can be estimated. The result is

$$\begin{aligned} \Delta_H &\approx 2S[J + (J_\perp + J'_\perp)(1 - \tilde{h}^2)]^{1/2} \\ &\times (J_\perp + J'_\perp)^{1/2}(1 - \tilde{h}^2)^{-1/2} \\ &\times \left[\left(1 - \frac{(J - J_\perp - J'_\perp)^2}{[J + (J_\perp + J'_\perp)\tilde{h}^2](J + J_\perp + J'_\perp)} \tilde{h}^2 \right)^{1/2} \right. \\ &\left. + \left(1 - \frac{J + J_\perp + J'_\perp}{[J + (J_\perp + J'_\perp)\tilde{h}^2]} \tilde{h}^2 \right)^{1/2} \right] \tilde{H} + \dots, \quad (\text{A12}) \end{aligned}$$

which is reduced to the conventional result $\Delta_H = H$ when $h = 0$. Both gaps have linear field dependence. The results (A11) and (A12) indicate that Δ_h (Δ_H) is nonvanishing only when $h \neq 0$ ($H \neq 0$). As a consequence, the true gap $\Delta = \min(\Delta_h, \Delta_H)$ is zero when either of h or H is zero.

2. The noncompetitive case

Here we summarize the spin-wave approximation on the noncompetitive case. We find that it can be straightforwardly applied also to the symmetric phase in the competitive case.

According to the MFT and Fig. 6, the spin configuration in the classical ground state can be written as

$$\vec{S}_{2n,j,k} \sim SR_y(-\theta)\hat{x}, \quad (\text{A13})$$

$$\vec{S}_{2n+1,j,k} \sim SR_z(\pi)R_y(-\theta)\hat{x}, \quad (\text{A14})$$

where \hat{x} is the unit vector pointing to x direction and θ is the canting angle parameter. The minimization of the classical energy determines $\theta = \theta_{\text{cl}}$ as

$$\cos \theta_{\text{cl}} \sin \theta_{\text{cl}} = \frac{H}{4SJ} \cos \theta_{\text{cl}} - \frac{h}{4SJ} \sin \theta_{\text{cl}}. \quad (\text{A15})$$

A standard spin-wave theory on this classical ground state gives the quadratic Hamiltonian in terms of bosons

$$\hat{H}_{\text{HP2}} = \sum_{\vec{k}} (a_{\vec{k}}^\dagger \ a_{-\vec{k}}) \begin{pmatrix} \frac{1}{2}A_{\vec{k}} & B_{k_x} \\ B_{k_x} & \frac{1}{2}A_{\vec{k}} \end{pmatrix} \begin{pmatrix} a_{\vec{k}} \\ a_{-\vec{k}}^\dagger \end{pmatrix} - \frac{1}{2}A_{\vec{k}} + \text{const}, \quad (\text{A16})$$

where

$$\begin{aligned} A_{\vec{k}} = A_{-\vec{k}} &= 2SJ \cos 2\theta_{\text{cl}} - 2SJ \sin^2 \theta_{\text{cl}} \cos k_x a_x \\ &+ 2S|J_\perp|(1 - \cos k_y a_y) \\ &+ 2S|J'_\perp|(1 - \cos k_z a_z) \end{aligned}$$

$$+ H \sin \theta_{\text{cl}} + h \cos \theta_{\text{cl}},$$

$$B_{k_x} = B_{-k_x} = -SJ \cos^2 \theta_{\text{cl}} \cos k_x a_x. \quad (\text{A17})$$

Now we apply the two-mode BT

$$\begin{pmatrix} a_{\vec{k}} \\ a_{-\vec{k}}^\dagger \end{pmatrix} = \begin{pmatrix} u_{\vec{k}} & v_{\vec{k}} \\ v_{\vec{k}} & u_{\vec{k}} \end{pmatrix} \begin{pmatrix} \tilde{a}_{\vec{k}} \\ \tilde{a}_{-\vec{k}}^\dagger \end{pmatrix}, \quad (\text{A18})$$

where $u_{\vec{k}}^2 - v_{\vec{k}}^2 = 1$, to Eq. (A16). The Hamiltonian is then diagonalized as

$$\hat{H}_{\text{HP2}} = \sum_{\vec{k}} \tilde{\omega}(\vec{k}) \tilde{a}_{\vec{k}}^\dagger \tilde{a}_{\vec{k}} + \text{const}, \quad (\text{A19})$$

if we choose $u_{\vec{k}}^2 = \frac{1}{2}(1 + A_{\vec{k}}/\tilde{\omega}(\vec{k}))$ and $v_{\vec{k}}^2 = \frac{1}{2}(-1 + A_{\vec{k}}/\tilde{\omega}(\vec{k}))$. The dispersion relation is given by

$$\tilde{\omega}(\vec{k}) = \sqrt{A_{\vec{k}}^2 - 4B_{k_x}^2}. \quad (\text{A20})$$

The above derivation and results apply exactly to the symmetric phase in the competitive case, only with the replacement $(|J_\perp|, |J'_\perp|) \rightarrow (-J_\perp, -J'_\perp)$. The dispersion (A20) has the gapless point $\tilde{\omega}(0,0,0)$ in the AF phase where $h = 0$. It corresponds to the NG mode due to the spontaneous breaking of the U(1) symmetry. Hence $\tilde{\Delta}_h = \tilde{\omega}(0,0,0)$ can be regarded as the h -induced gap. At the small field h , the angle variation around $h = 0$: $\delta\theta \equiv \sin^{-1}(H/4JS) - \theta_{\text{cl}}$ is estimated approximately as

$$\delta\theta \approx -\frac{H}{(4SJ)^2 - H^2} h. \quad (\text{A21})$$

Therefore expanding $\tilde{\Delta}_h^2(h, \delta\theta)$ around $h = \delta\theta = 0$, one sees that the gap grows as

$$\tilde{\Delta}_h \approx \sqrt{4SJ} \left[1 - \left(\frac{H}{4SJ} \right)^2 \right]^{1/4} \left[1 + 2 \left(\frac{H}{4SJ} \right)^2 \right]^{1/2} h^{1/2}. \quad (\text{A22})$$

In contrast to the SSB phase (in the competitive case), the h -induced gap opens as $\tilde{\Delta}_h \propto h^{1/2}$. Furthermore, it is remarkable that Eq. (A22) has no dependence on the interchain interactions. In fact, it is identical to the 1D result [Eq. (3.17) in Ref. 5]. This is a reflection of the smoothness which was discussed in the final of Sec. III. At $H = 0$, we can obtain the simple exact result $\tilde{\Delta}_h = \sqrt{4SJh} [1 + h/(4SJ)]^{1/2}$ from the dispersion (A20).

¹M. Oshikawa and I. Affleck, Phys. Rev. Lett. **79**, 2883 (1997).

²Y.-J. Wang, F.H.L. Essler, M. Fabrizio, and A.A. Nersisyan, Phys. Rev. B **66**, 024412 (2002).

³I. Dzyaloshinsky, J. Phys. Chem. Solids **4**, 241 (1958).

⁴T. Moriya, Phys. Rev. **120**, 91 (1960).

⁵I. Affleck and M. Oshikawa, Phys. Rev. B **60**, 1038 (1999); **62**, 9200 (2000).

⁶D.C. Dender, P.R. Hammar, D.H. Reich, C. Broholm, and G. Aeppli, Phys. Rev. Lett. **79**, 1750 (1997).

⁷T. Asano, H. Nojiri, Y. Inagaki, J.P. Boucher, T. Sakon, Y. Ajiro,

- and M. Motokawa, Phys. Rev. Lett. **84**, 5880 (2000).
- ⁸T. Asano, H. Nojiri, W. Higemoto, A. Koda, R. Kadono, and Y. Ajiro, J. Phys. Soc. Jpn. **72**, 594 (2002).
- ⁹R. Feyerherm, S. Abens, D. Günther, T. Ishida, M. Meißner, M. Meschke, T. Nogami, and M. Steiner, J. Phys.: Condens. Matter **12**, 8495 (2000).
- ¹⁰M. Oshikawa, K. Ueda, H. Aoki, A. Ochiai, and M. Kohgi, J. Phys. Soc. Jpn. **68**, 3181 (1999).
- ¹¹H. Shiba, K. Ueda, and O. Sakai, J. Phys. Soc. Jpn. **69**, 1493 (2000).
- ¹²M. Kohgi, K. Iwasa, J.M. Mignot, B. Fak, P. Gegenwart, M. Lang, A. Ochiai, H. Aoki, and T. Suzuki, Phys. Rev. Lett. **86**, 2439 (2001).
- ¹³In general it is possible that there are more complex forms of the g tensor and the DM interaction than Eqs. (1) and (2). The forms of Eqs. (1) and (2) are almost consistent with ones of Cubenzoate, $[\text{PM} \cdot \text{Cu}(\text{NO}_3)_2 \cdot (\text{H}_2\text{O})_2]_n$ and Yb_4As_3 .
- ¹⁴F.C. Alcaraz and A.L. Malvezzi, J. Phys. A **28**, 1521 (1995).
- ¹⁵M. Oshikawa and I. Affleck, Phys. Rev. Lett. **82**, 5136 (1999).
- ¹⁶M. Oshikawa and I. Affleck, Phys. Rev. B **65**, 134410 (2002).
- ¹⁷A. Zheludev, E. Ressouche, S. Maslov, T. Yokoo, S. Raymond, and J. Akimitsu, Phys. Rev. Lett. **80**, 3630 (1998).
- ¹⁸S. Maslov and A. Zheludev, Phys. Rev. B **57**, 68 (1998).
- ¹⁹C.P. Landee, A.C. Lamas, R.E. Greeney, and K.G. Bücher, Phys. Rev. B **35**, 228 (1987).
- ²⁰Dan Reich (private communication); Y. Cheng, Ph.D thesis, Johns Hopkins University, 2002.
- ²¹M. Kenzelmann, Y. Chen, C. Broholm, D.H. Reich, and Y. Qiu, cond-mat/0305476.
- ²²T. Yamada, Z. Hiroi, and M. Takano, J. Solid State Chem. **156**, 101 (2001).
- ²³D.J. Scalapino and Y. Imry, Phys. Rev. B **11**, 2042 (1975).
- ²⁴H.J. Schulz, Phys. Rev. Lett. **77**, 2790 (1996).
- ²⁵T. Holstein and H. Primakoff, Phys. Rev. **58**, 1098 (1940).
- ²⁶J.H.P. Colpa, Physica A **93**, 327 (1978).
- ²⁷When the staggered field which is *parallel* to the uniform field is applied in the $S=1/2$ XXZ chains, there exists a possibility that the staggered field does not induce gaps. For details, see Ref. 14.
- ²⁸Z. Wang, Phys. Rev. Lett. **78**, 126 (1997).
- ²⁹I. Affleck, in *Champs, Cordes et Phenomenes Critiques; Fields, Strings and Critical Phenomena*, edited by E. Brézin and J. Zinn-Justin (Elsevier, Amsterdam, 1989), p. 564.
- ³⁰*Bosonization*, edited by M. Stone (World Scientific, Singapore, 1994).
- ³¹A.O. Gogolin, A.A. Nersesyan, and A.M. Tsvelik, *Bosonization and Strongly Correlated Systems* (Cambridge Univ. Press, Cambridge, England, 1998).
- ³²J.L. Cardy, *Scaling and Renormalization in Statistical Physics* (Cambridge Univ. Press, Cambridge, England, 1996).
- ³³H.J. Schulz, G. Cuniberti, and P. Pieri, in *Field Theories for Low-Dimensional Condensed Matter Systems*, edited by G. Morandi *et al.* (Springer, New York, 2000).
- ³⁴V.E. Korepin, N.M. Bogoliubov, and A.G. Izergin, *Quantum Inverse Scattering Method and Correlation Functions* (Cambridge Univ. Press, Cambridge, England, 1993).
- ³⁵S. Eggert, I. Affleck, and M. Takahashi, Phys. Rev. Lett. **73**, 332 (1994).
- ³⁶S. Lukyanov and A. Zamolodchikov, Nucl. Phys. B: Field Theory Stat. Syst. **493[FS]**, 571 (1997).
- ³⁷S. Lukyanov, Mod. Phys. Lett. A **12**, 2543 (1997).
- ³⁸I. Affleck, M.P. Gelfand, and R.R.P. Singh, J. Phys. A **27**, 7313 (1994).
- ³⁹I. Affleck and B.I. Halperin, J. Phys. A **29**, 2627 (1996).
- ⁴⁰A.W. Sandvik, Phys. Rev. Lett. **83**, 3069 (1999).
- ⁴¹I. Tsukada, J. Takeya, T. Masuda, and K. Uchinokura, Phys. Rev. Lett. **87**, 127203 (2001).